Multifunctional tribometer development and performance study of CuCrZr-316L material pair for ITER application

Julien Hillairet, Z.X. X Chen, Viviane Turq, Y.T. T Song, Raphaël Laloo, K. Vulliez, J.M. M Bernard, Q.X. X Yang, C. Hernandez, L. Ferreira, et al.

This is an author's version published in: http://oatao.univ-toulouse.fr/24499

Multifunctional tribometer development and performance study of CuCrZr-316L material pair for ITER application

Z. Chen [a,*], J. Hillairet [a], V. Turq [b], Y. Song [c], Q. Yang [c], G. Lombard [a], K. Vulliez [d], P. Mollard [a], R. Volpe [a], J.M. Bernard [a], C. Hernandez [a], F. Ferlay [a], S. Larroque [a], R. Laloo [b], V. Bruno [a], J.C. Hatchressian [a], H. Xu [c]

[a] *CEA, IRFM, F-13108 Saint-Paul-Lez-Durance, France*
[b] *Institut Carnot CIRIMAT, UMR CNRS-UPS-INP 5085, Université Paul-Sabatier, 118 Route de Narbonne, 31062 Toulouse Cedex 9, France*
[c] *Institute of Plasma Physics, CAS, Hefei, Anhui 230031, PR China*
[d] *Laboratoire d'étanchéité, DEN/DTEC/SDTC, CEA, 2 Rue James Watt, 26700 Pierrelatte, France*

ABSTRACT

Radio-Frequency (RF) contacts are key components on the International Thermonuclear Experimental Reactor (ITER) Ion Cyclotron Resonance Heating (ICRH) antenna, and these components are facing big challenges such as 2 kA operation current load and intensive sliding under up to 250 °C in high vacuum. Stainless steel (SS) 316L and CuCrZr are most likely to be applied as base materials for the conductor and the RF contacts louvers. To evaluate the performance of the selected materials, their electrical and tribological behaviors have to be studied. A multifunctional tribometer which can mimic the ITER ICRH RF contacts' relevant working conditions was designed and built in CEA. The contact resistance (Rc) and coefficient of friction (CoF) of CuCrZr-316L pair were researched on this tribometer.

1. Introduction

ITER is the world largest fusion experimental facility which is being constructed in France to demonstrate the feasibilities of using fusion as an energy source [1]. In order to heat the deuterium and tritium fuel to fusion temperatures, two sets of ICRH systems with total heating power of 40 MW (40 55 MHz) are anticipated to be applied [2,3]. Transmission lines are designed on the ICRH antenna whose function is to transfer the RF power from the RF generators far from the ITER machine to the ITER plasmas. In order to ease the ICRH antennas' assembly, enhance the maintainability, realize radial sliding and release thermal stresses, few flexible electrical contacts (RF contacts) will be installed on the RF transmission lines [3 5]. During operation, these RF contacts will be working under high temperature (>130 °C) and high vacuum (<10^{-3}Pa), and one of the RF contacts is designed to be operated under the current of 2 kA with current density of 4.8 kA/m [2,6]. In addition, wear phe nomenon will occur on the RF contact louvers during operation. The harsh working conditions of the RF contacts lead to a high demand on the RF contact materials' properties, such as mechanical strength especially under high temperature and neutron radiation, resistivity and thermal conductivity.

In the lifetime of ITER, the machine components will be baked for outgassing at 250 °C during an estimated time of 850 days. Copper is an interesting material with high electrical conductivity, however, creeping issues make it unsuitable as contact louver material [6]. On the Large Hadron Collider (LHC) RF contact which works under the nominal beam current of 0.6A, CuBe was applied to manufacture the contact fingers [7,8]. While, for ITER RF contacts which are expected to be operated under 2 kA, the high resistivity and relative low thermal conductivity of CuBe make it improper to be used. CuCrZr alloy belongs to the group of alloys that have high electrical conductivity and moderately high toughness. Consequently they are suitable for high loading parts under electrical current such as springs, contact wheel, etc. [9]. On ITER, the CuCrZr is presently widely used on the plasma facing components exposed to high heat flux during operation [10 13]. Thus, CuCrZr has already been selected as a base material for the ITER ICRH RF contact louvers' manufacturing.

As a sliding electrical contact, the contact louvers whose base

---

material is CuCrZr will be slid against the RF conductor made of SS 316L. The sliding contact performance especially the evolution of Rc and CoF with sliding cycles and wear phenomena of the two surfaces under ITER relevant conditions should be well studied. A dedicated multifunctional tribometer: Heatable Vacuum Material Tribiogical & Electrical Study Testbed (HV MTEST) was developed successfully in CEA (France) to carry out such studies. In this paper, the engineering design of this test bed and the electrical/tribological performance tests of CuCrZr versus SS 316L are presented.

2. HV-MTEST system design and simulation

2.1. Overview

The tribological characterizations are aimed at determining friction and wear behaviors of the studied material pairs under ITER relevant vacuum and thermal conditions, which include: vacuum lower than 10^{-3}Pa and temperature higher than 130 °C. For CoF experimental study, the tribometer type should be adapted and reveal the real studied com ponents' configuration and their relative motions as much as possible to improve the relevancy of the results. Generally speaking, there are six main types of tribometers existing [14], with the most commonly used on commercial tribometers are pin on plate, pin on disc and ball on disc. For ITER ICRH RF contacts, during shimming or thermal induced movement, the RF contact fingers will be linearly sliding against the conductor reciprocally under low sliding speed. Therefore, the structure configu ration of pin on flat with reciprocating motion was finally selected for the HV MTEST design. Actually, reciprocating sliding concept can simplify the high vacuum sealing structure, which can be realized by using bellows.

The design specifications of the HV MTEST are shown in Table 1.

As Fig. 1 shows, the HV MTEST facility consists of six sub systems: the CoF measurement system based on full bridge gauge circuit; the normal loading system; the high vacuum/baking system; the motor drive system that allows the reciprocating sliding; the data acquisition & controlling system and the Rc measurement system based on four terminal method. The main novelties of the proposed multifunctional tribometer machine design lie in its ability to directly control the normal force by adding standard dead loads gradually from outside of the vacuum vessel without breaking the vacuum, the realistic ITER ICRH RF contact working envi ronment simulation, and the precise static measurement of the Rc or dynamic simultaneous measurements of the CoF and Rc.

2.2. CoF measurement system

The instantaneous CoF (μ) is defined as the ratio of the friction force (F_f) and the normal contact force (F_n) which is expressed as:

$$\mu = \frac{F_f}{F_n}$$

Force sensors are the most important and critical elements for accu rate tribological measurements which have to respond to some important criteria, like vacuum compatibility, accuracy and repeatability [15]. Even though the calibration procedure is mandatory for the tribometer user and it is usually performed well in the atmosphere condition before

Table 1
Design specifications of the HV-MTEST.

Parameter	value
Normal contact force	6N-30 N
Sliding speed	0-10 mm/s
Stroke	±20 mm (Max)
Operating temperature	Room temperature-250 °C (steady-state)
	250 °C −350 °C short period
Vacuum	1 atm-10 ^{5}Pa

the tests, for the high temperature and high vacuum tribometer, due to the thermal and pressure effects, misalignment of the force measurement sensors could be generated. However, the new calibration of the sensors under the exact same conditions as the real tests is time consuming and for most vacuum working conditions it's impossible. Typically, a cali brated force transducer or sensor that results in a measurable response when subjected to friction is commonly used to measure the friction force, and such sensors include strain gauges, spring sensors [16], piezoelectric force sensor [14] and S2M load cell [17]. In order to handle the high temperature baking and high vacuum application requirements, strain gauges with nickel chromium alloy grid, encapsulated in fiberglass reinforced epoxy phenolic and Teflon insulated connecting wires were selected which can be operated under 260 °C steadily.

As Fig. 2 shown, the main component of the CoF measurement system is the cantilever beam which is supported by two ball bearings and a central shaft. To avoid the self loading by the gravity force of the canti lever beam to the test samples, a counterweight load is designed to keep its balance. The friction force is measured indirectly by measuring the bending strain caused by the bending moment, and a necking part on the cantilever beam is designed to increase the sensitivity. In order to lower outgassing rate and make it high vacuum compatible, all the parts were made of SS 304 with mechanical polishing and grease cleaning. Accurate measurement of small changes in resistance is critical in case of strain gauge application and Wheatstone bridge offers a good method for small strain measurement [18]. On HV MTEST, four working gauges are used which are point welded on the two surfaces of the necking part of the cantilever beam symmetrically and then connected in a full bridge Wheatstone circuit. The main advantage to use such a full bridge cir cuit is: improving the sensitivity of the gauge system by amplifying the output voltage to four times than the quarter bridge. The resistances of the lead wire and the temperature induced resistance change can be compensated internally in the full bridge, which improves the accuracy of the system. The Rc is measured by using four terminal resistance measurements method. The pin sample (with its holder) and the plate sample are insulated with other components by Al_2O_3ceramic plates.

2.3. Loading system

Loading system is designed to apply a constant and stable contact force between the pin and flat samples during sliding. Few techniques can be used to apply the contact force such as dead weight, springs, hydraulic systems, etc. Except for the dead weight, almost all the other methods require calibration for the system itself or for the force trans ducers to acquire good precision for contact force measurement. As HV MTEST is designed for high temperature application, so the unpredict able thermal effects on the sensors is difficult to be eliminated. Actually, dead weight loading is the most reliable, cheapest and simplest to implement and was chosen on HV MTEST eventually.

For ITER ICRH RF contact, the contact force is an important param eter which has strong effects on the Rc, CoF and wear rate. Therefore, it needs to be investigated carefully. For the classical tribometers working under ambient atmosphere, the change of contact force can be realized by adding or removing loads manually. However, on a vacuum trib ometer like HV MTEST, the load change is complicated due to the high vacuum test conditions. Indeed, breaking the high vacuum and changing the dead weight is really time consuming. To simplify the loading pro cess, an innovative system was designed as shown in Fig. 3. Five load plates made of CuCrZr (6N/load plate) are connected in series by sixteen hocks and on each of the load plate four lifting points are mounted to keep the balance of the plates horizontally. The whole load plate as sembly is driven by a screw nut mechanism manually from the outside of the vacuum vessel with the vacuum insulation by a bellows. The loading process can be monitored from an observation window. With this flexible loading system, the contact force can be increased from 6 N to 30 N (with 6 N/step) conveniently without breaking the vacuum.
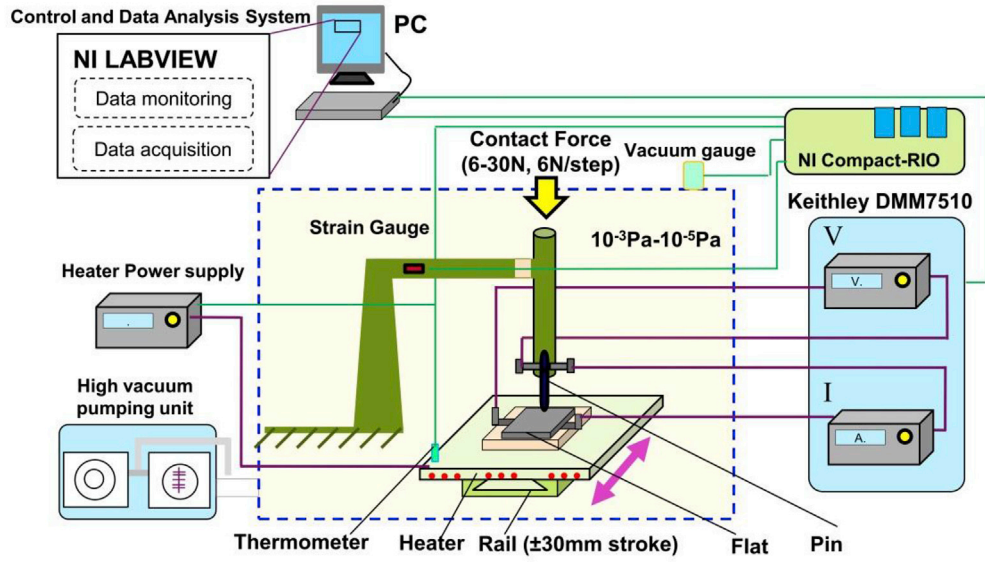
Fig. 1. Scheme of the HV-MTEST facility.
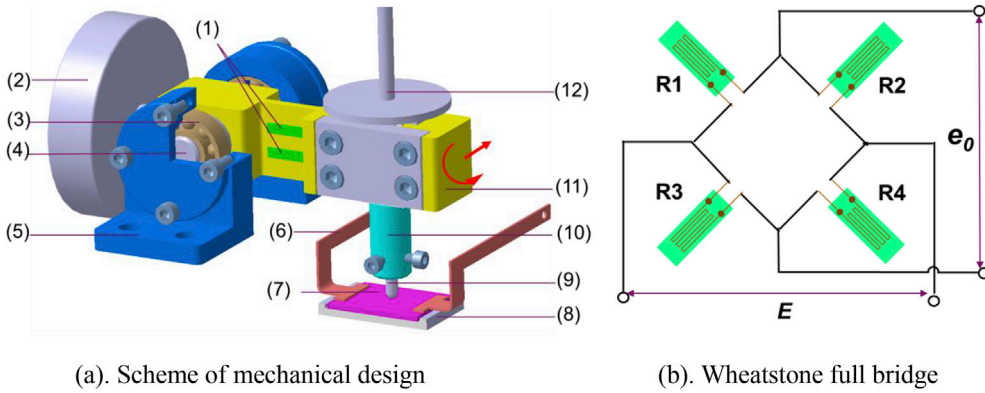
(a). Scheme of mechanical design

(b). Wheatstone full bridge

Fig. 2. Design of the CoF measurement system: (1). Strain gauges (× 4); (2). Counterweight; (3). Bearings (× 2); (4). Central shaft; (5). Beam support; (6). Electrodes (× 2); (7). Plate sample; (8). AlN ceramic plate; (9). Pin sample; (10). Pin sample holder; (11). Cantilever beam; (12). Loading support.

Fig. 3. Loading system of the HV-MTEST: (1). Load lifting mechanism; (2). Al_2O_3 insulation joint; (3). Dead load support; (4). Dead load plates (6 N × 5); (5). Hocks (× 16).

2.4. Vacuum and baking system

As the HV MTEST is designed for the operation under high vacuum level, therefore a high vacuum pumping set consisted of a turbo molecular pump and a backing diaphram pump was selected (Fig. 4). Considering the vibration of the pumping set during operation may induce the ground noise of the strain gauge measurement system, a bellows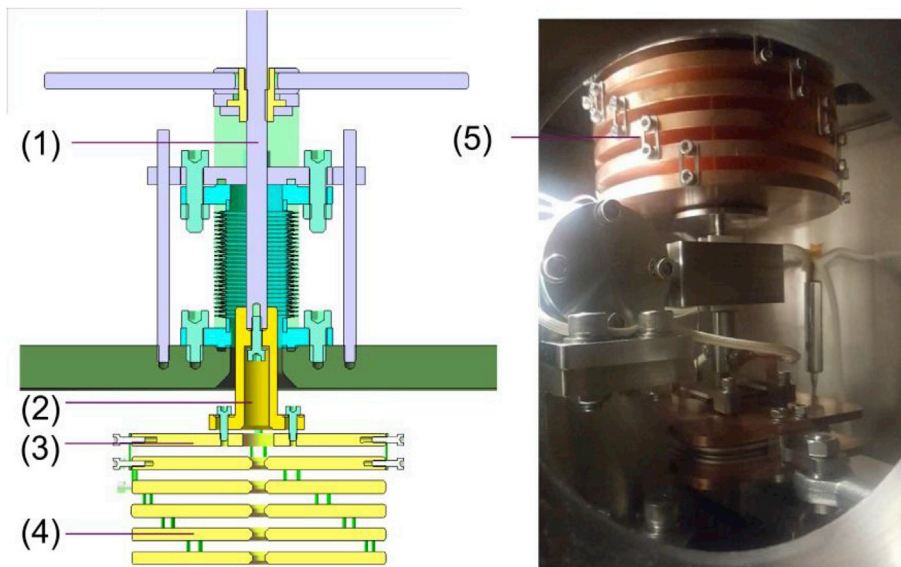 is installed between the pump set and the vacuum tank of the HV MTEST even though it can abate the pumping efficiency of the pump set. There are two heaters installed, one is integrated on the sample holder plate to bake the samples to reach the expected test temperature and the other is attached around the vacuum vessel to accelerate the outgassing process and to improve the vacuum by heating the whole tank up to 150 °C. The vacuum of the HV MTEST could also be improved if needed by changing the gasket from FKM to metallic seal.

2.5. Motor drive system

Reciprocating sliding is selected as the HV MTEST motion type, under which the main part of the drive system like the guide rods, motor, bearing and coupling can be installed outside of the vacuum tank of the tribometer, and the linear motion is transmitted to the vacuum chamber through a shaft sealed by bellows. An Alternating Current (AC) servo motor is used to serve the rotation. The motion transfer from the motor's rotation to the shaft's linear sliding is realized by a screw nut mechanism with two horizontal guide rods. To compensate the axis misalignment between the motor and the central shaft, a flexible coupling is installed. Even though most of the drive system parts which need oil lubricate is placed outside of the vacuum tank, a rail in the vacuum tank that makes the sample holder plate slide steadily is required. A high vacuum compatible and high precision ball linear guide is used.

2.6. Data acquisition and controlling system

A National Instrument Compact RIO which incorporates a real time processor and reconfigurable FPGA has been setup for the control and acquisition system [19]. A PC with LabVIEW is dedicated to data acquisition and monitoring and a NI Compact RIO 9002 controller is connected with the PC through ethernet.

The two channels of temperature signals are collected by the thermocouple input module NI 9211, and the heaters can be controlled by the temperature regulator (PID controller) precisely with the error of ±0.5 °C. The signals of the strain gauge full bridge are acquired by a 24 bit full bridge module (NI 9237) and the vacuum gauge signal is acquired by the NI9201. The motor is controlled by its own controlling system and is setup through the self developed graphical user interface. Single or periodic sliding can be programmed at a velocity varying between 0 and 10 mm/s. The stroke of the plate is defined within (up to) ±20 mm.

2.7. Modeling and simulations results

The finite element method (FEM) is an essential solution technique for engineering design, which can help to understand the structure's behavior under exact loads so as to evaluate the structure's safety or functional performance. During the design of HV MTEST, ANSYS software was used to analyze the key components' mechanical behaviors under friction force, and their structure optimizations were performed based on such results.

Since the cantilever beam is the key component for the CoF measurement, which has strong effect to the sensitivity of the strain gauges. For sensitivity consideration, the thickness of the necking part should be as thin as possible, and by applying a small force (friction force), the bending phenomenon of this part could be obvious strong enough to generate a significant output for the Wheatstone full bridge. Meanwhile, robust structure of the necking part should be guaranteed to avoid any plastic deformations. Beside the controlling the necking part thickness, designing a rigid supporting structure for the cantilever beam to avoid large elastic deformation on the supporting structure during the CoF measurement tests is another solution to improve the sensitivity of the measurement system. The concept of the CoF measurement is based on the direct measurement of the bending strain on the necking part caused by the friction force, however, except for the bending moment, there is also a torque applied on the cantilever beam (Fig. 1). Actually, the final strain on the necking part is the combined effect of the bending moment
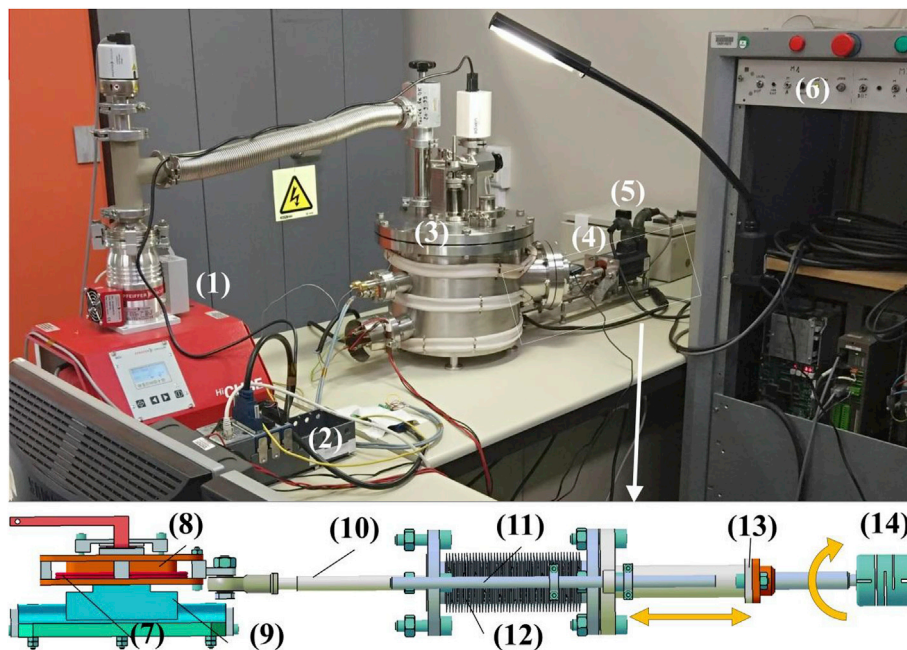

Fig. 4. A photograph of the HV-MTEST assembly: (1). High vacuum pumping set; (2). NI cRIO-9002; (3). Vacuum tank with heaters; (4). Motor drive system; (5). Temperature regulator; (6). Motor controlling system; (7). Sample heater; (8). Sample holder plate; (9). Ball linear guide; (10). Central shaft; (11). Guide rods; (12). Bellows; (13). Screw nut mechanism; (14). Flexible coupling.
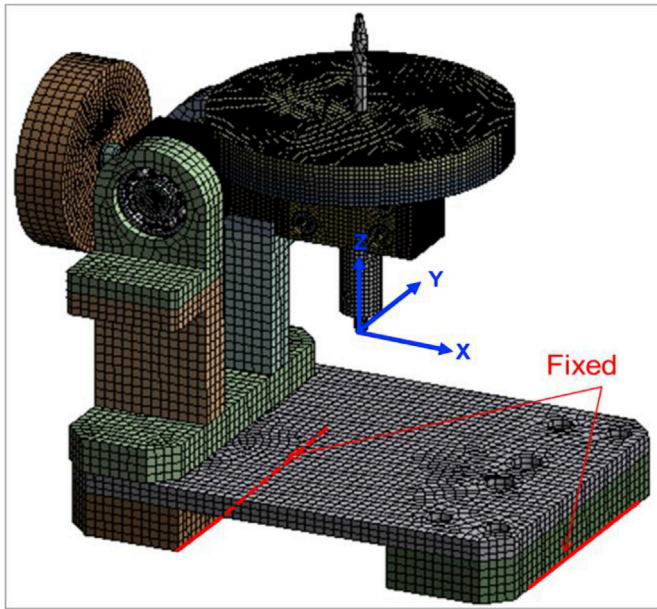
Fig. 5. FEM and meshing of the HV-MTEST.

and the torque. The concept of the Wheatstone full bridge measurement is based on the hypothesis that the four strain gauges would have the same elastic deformation. So, choosing an area on the necking part where strain is uniformly distributed for the gauge attachment is meaningful to improve the linear relationship between friction force and strain measured from the full bridge. The application of FEM analysis of the cantilever beam can help to solve the above problems.

A simplified model of the HV MTEST main in vessel components was created as shown in Fig. 5, and in this model, the thickness of the necking part was original designed as 4 mm. The friction force was applied at the tip of the pin along Y direction, and the bottom support plates were fixed. The maximum contact force of the HV MTEST was 30 N, and the maximum CoF between the test samples was assume as 2 (includes a safety margin), then the maximum friction force was calculated as 60 N. The strain and stress distribution on the necking part and the cantilever beam support are shown in Fig. 6.

Under friction force of 60 N, the maximum strain generated on the cantilever beam is 0.0463%, which occurs at the thickness transition position. In the middle of the necking part, the strain is about 0.02%. The maximum strain is observed on the beam support and is only 0.00126% which shows that the support structure has good stiffness. Under 60 N, the maximum stress on the cantilever beam is about 92.4 MPa and such value is lower than the yield stress of the SS 304 under 350 °C whose value is 103 MPa [20]. So, the structure can be operated under 350 °C steadily without any plastic deformation. It is also shown that, the relative uniform distribution area of the strain on the necking part is the middle area, so in the strain gauge welding process, the gauges should be installed as near as possible to the center of the necking part.

Although the static stress on the tribometer structure is less than the material's mechanical strength, rapture still may occur due to repeated application of stresses which induce fatigue failure [21]. For HV MTEST, the critical component that subjects to fatigue failure is the cantilever beam on which a necking part was designed. The fatigue loading of the cantilever beam is the friction forces that are intended to be measured. The life time of HV MTEST is expected to be higher than 2×10^5 cycles, which indicates that the fatigue of the cantilever beam belongs to high cycle fatigue situation [22]. Under friction force of 60 N, the maximum strain on the cantilever beam is 0.0463%, and by checking the strain allowable cycles curve, the life time of the cantilever beam is higher than 10^8 cycles [23]. No fatigue failure anticipated on the HV MTEST facility.

3. Calibration of the CoF measurement

Since the friction force between samples can't be measured directly, instead it's deduced from the strain occurs on the cantilever beam. In order to find the corresponding friction force which results in the strain, the inherent relationship between the friction force and strain on the cantilever beam's necking part should be investigated. Such relationship is determined by the configuration of the beam design. For the cantilever beam with rectangle cross section, the bending strain can be theoretically calculated by the equation:

$$\varepsilon = \frac{6FL}{bh^2E}$$

where F is bending force applied on the cantilever beam, L is the distance between the strain gauge center to the load position (0.0385 m), b is the width of the cantilever beam (0.03 m), h is the thickness of the cantilever beam (0.004 m), E is the Young's modulus of the SS304 (200 GPa). The bending strain corresponds the bending force is plotted in Fig. 7 (a).

Unlike the common way to attach strain gauges, the high temperature strain gauges applied in this study were point welded on the cantilever beam at the edge areas other than glued totally. Therefore, the difference between the strains that occur on the strain gauge and on the cantilever beam is unavoidable, and the latter one is larger. So, several calibration procedures were performed after manufacturing and assembling to investigate the relationship between the friction force and the strain outputted from the grain gauges. The calibration system is shown in Fig. 7 (b), in which the friction forces were simulated by applying a series of dead loads with different weight (0.38 N, 0.52 N, 1.23 N, 2.07 N), and the strain responses of the cantilever bean were recorded. After measurement, the least squares method was used to do the linear fitting and the final expression of strain corresponding to friction force is:

$$\varepsilon = 0.086 + 1.998F_f \left(\times 10^{-6} \right)$$

So, the friction force F_f that the applying on the pin during sliding can be calculated from the bending strain from the equation of:

$$F_f = 0.043 + 0.5\varepsilon (N)$$

The calibration results show that, the HV MTEST has very good linearity property between the input of friction force and the output of strain.

4. Electrical and tribological performance study of CuCrZr-316L sliding pair

The value of CoF is an important parameter to calculate the insertion force of the ITER RF contact components by remote handling. The estimation of the Rc is mandatory to estimate the thermal behavior of the contact when the RF current flowing through the contact interface. The Joule heat generated on the RF contact by RF current is directly linked to the R_C value. Under steady state operation, the RF contact's temperature raise may lead to failure and destruction. Classical contact theory indicates that between two macro contacting surfaces the real contact areas are established between clusters of micro asperities referred as a spots [24]. When the contact force increases, the a spots area becomes larger and new a spots are formed, which decrease the Rc accordingly [25]. Under high temperature such effect is more obvious since the materials' hardness is low. Meanwhile, the Rc changing rate decreases with the contact force increase, which means that the Rc will not be sensitive anymore to the contact force increase when the contact force becomes relatively high. Under high contact force, the asperities on the contacting surfaces can plunge into each other and therefore the adhesive bonding between the two surfaces' materials strengthened, which accelerates the abrasion at the contacting interface. So, finding the proper value of contact force for the ITER ICRH RF contact by taking into account the
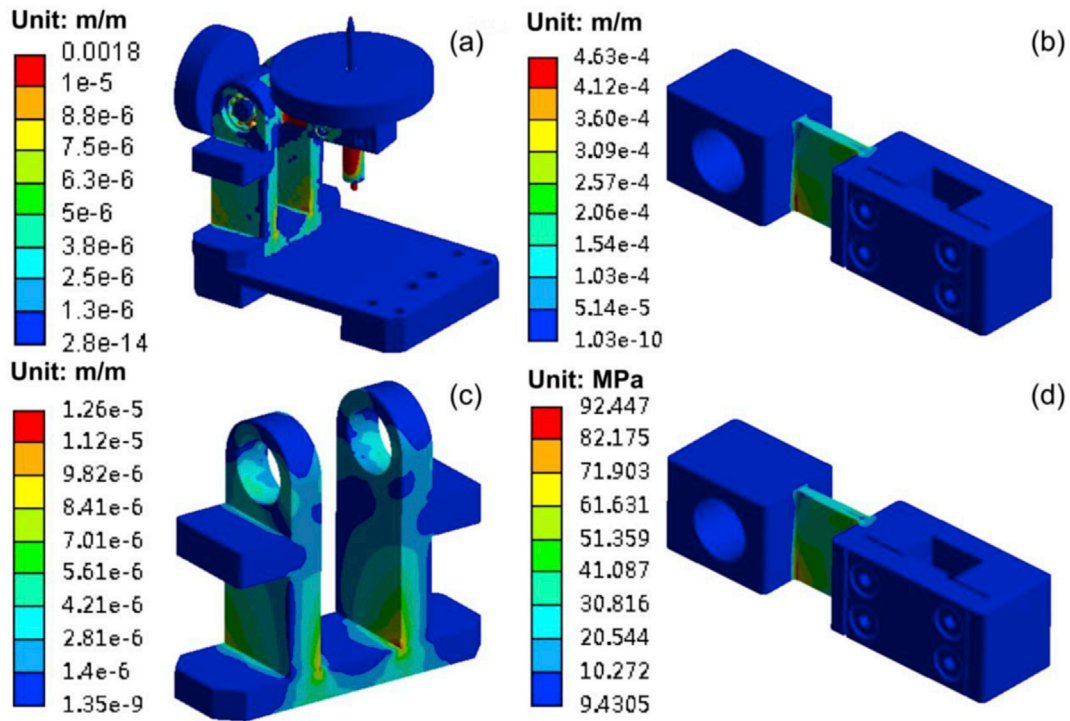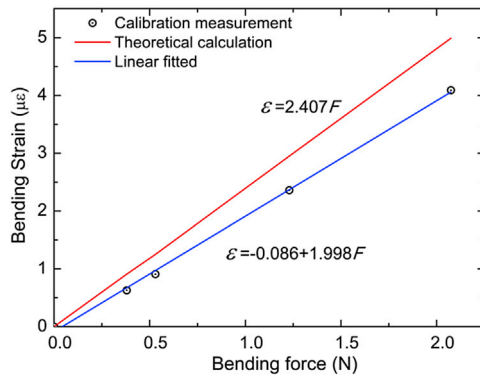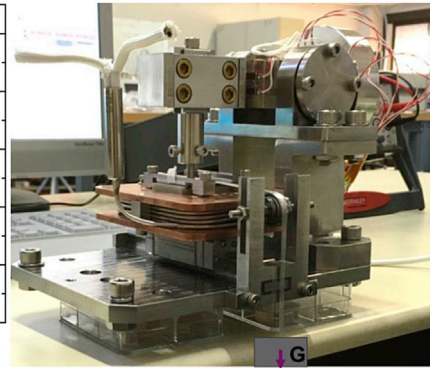
Fig. 6. Structural analysis results: (a). Global strain distribution; (b). Strain distribution on the cantilever beam; (c). Strain distribution on the support; (d). Stress distribution on the cantilever beam.

(a). F_f–ε relation of the HV-MTEST (b). Scheme of calibration

Fig. 7. Calibration of the HV-MTEST.

component's electrical and mechanical performance (including wear) is a very important work for the mechanical design. The dynamic changes of the Rc and CoF during reciprocating linear sliding are expected to be obtained to evaluate the ITER ICRH RF contact's lifetime.

4.1. Material and sample preparation

The samples used in this study are shown in Fig. 8. The plate samples are made of SS 316L with the sizes of 40 mm × 30 mm × 2 mm. The pins are made of CuCrZr ((ASTM C18150), Cr: 0.7 wt%, Zr:0.04 wt%, Cu: the rest) and they are cylinders with length of 25 mm and diameter of 5 mm. On the tip of the pin, a spherical surface with radius of 8 mm was designed which acts as the contact surface against the plate sample. The roughness of the pin and plate was characterized by using a 3D optical profiler (SENSOFAR, USA), and the values (Sa) are 2.1 μm and 0.45 μm respectively. All the samples were cleaned and rinsed with ethanol before the tests to clean the organic pollution.
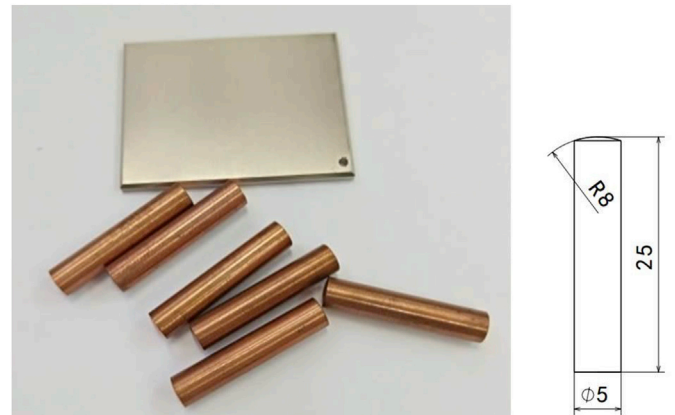

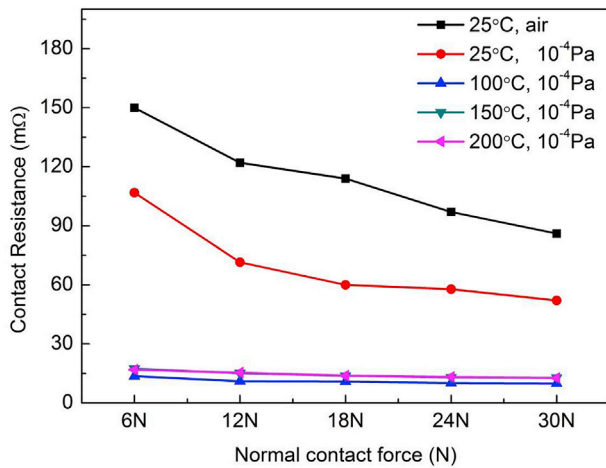**Fig. 8.** Configuration of test samples used on HV-MTEST.

Fig. 9. Rc measurement results under different contact force and temperature.

4.2. Static contact resistance measurement

The effects of vacuum condition, operation temperature and normal contact force to the Rc were studied on HV MTEST. Generally, when the normal contact force is applied, the process of elastic and plastic deformation between the asperities on the contacting surfaces can finish in a short time and the value of Rc turns to static quickly. However, for the CuCrZr SS316L pair, during the static contact resistance measurements, after the loads being applied, the value of Rc varied all the time and it's hard to achieve the steady state. The reason of the Rc instability is probably caused by the oxidation on the surface of CuCrZr pin, which behaves like insulation layers between two electrical contact surfaces. The oxidation phenomenon of CuCrZr had been well researched and the oxidations are Cu_2O and CuO [26,27]. As Fig. 9 shows, under room temperature, the significant effect of high vacuum ($\sim 10^{-4}$Pa) to decrease the contact resistance was approved. Under the same contact forces, the Rc under high vacuum were about 50 mΩ lower than those measured under in air. This phenomenon was caused by the release of gases and greases physically absorbed on the pin tips.

Increasing contact force can enlarge the real contact area and break the copper oxidation layers, as a result, the Rc decreased. However, the obvious effect of normal contact force to the Rc was only observed when the operation temperatures were lower than 100 °C, and its effect weakened after 18 N. Under 6 N, when the operation temperature was higher than 100 °C, the Rc decreased by one order of magnitude, which stabilized at around 15 mΩ. This sharp decrease of Rc was mainly due to the decomposition of the grease under high temperature and the obvious improvement of contact quality caused by plastic deformation of the contact materials under high temperature. Beyond 100 °C, the Rc was not sensitive to the temperature increase and the normal contact force increase neither. In addition to the effects such as pollution removal and contact area enlarging, increasing the operation temperature can increase the resistivity of the contact materials as well. As a result, under the same normal contact forces, the Rc at 150 °C and 200 °C were higher than those at 100 °C.

4.3. Evolution of Rc and CoF during sliding cycles

CoF is most often as a function of three main influencing parameters: the temperature, slip speed, and normal force [14,28]. Although for the ITER ICRH RF contact, the normal operation temperature is hard to be predicted, which is constrained by the RF contact's mechanical structure, cooling design, as well as the thermal deposition. For the material performance study, the operation temperature of 200 °C was used as the estimated value to simulate the realistic operating temperature conditions. Based on the results from section 4.2, at 200 °C the Rc was not sensitive to the normal contact force and after 18 N, there almost no change for the Rc. Poor contact may induce arcing and melting on the RF contacts, so 18 N was selected in the sliding test to guarantee the electrical contact's stability. The sliding speed of the plate sample was 1 mm/s and the vacuum was around 7×10^{-4}Pa. 2000 cycles of sliding test under the above conditions with sliding stroke of 16 mm was performed. The transient results of the Rc and CoF are shown in Fig. 10.

At the beginning of the sliding, the contact surface was smooth so the CoF was about 0.1. Before 200 cycles, the CoF was only slightly changed from 0.12 to 0.15. After 220 cycles, the CoF started to change faster, and the CoF reached to 0.25 at nearly 700 cycles. The maximum value of CoF occurred at around 1400 cycles and reached to 0.3. While, for the Rc, the
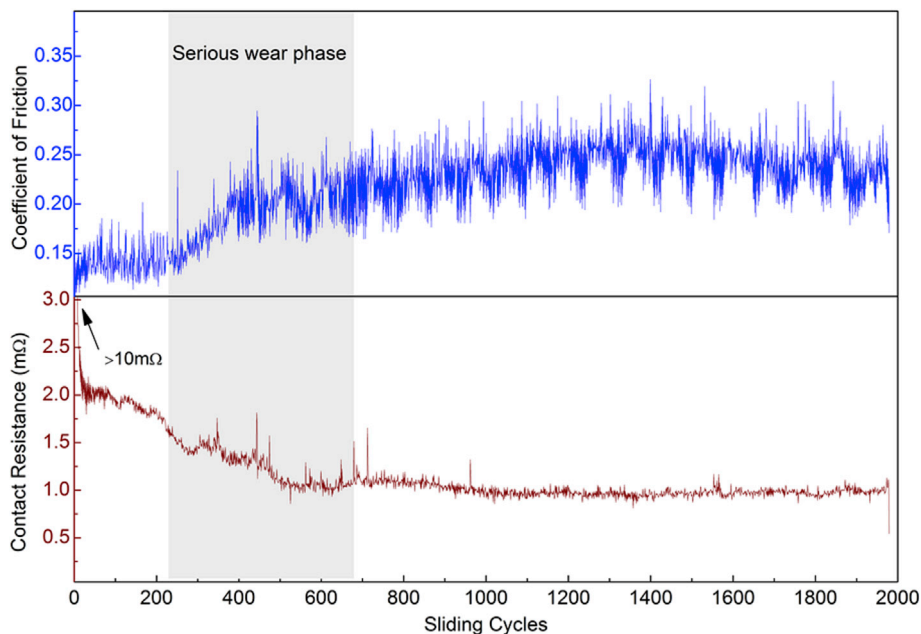

Fig. 10. Evolution of the Rc and CoF under the 2000 cycles of sliding tests.
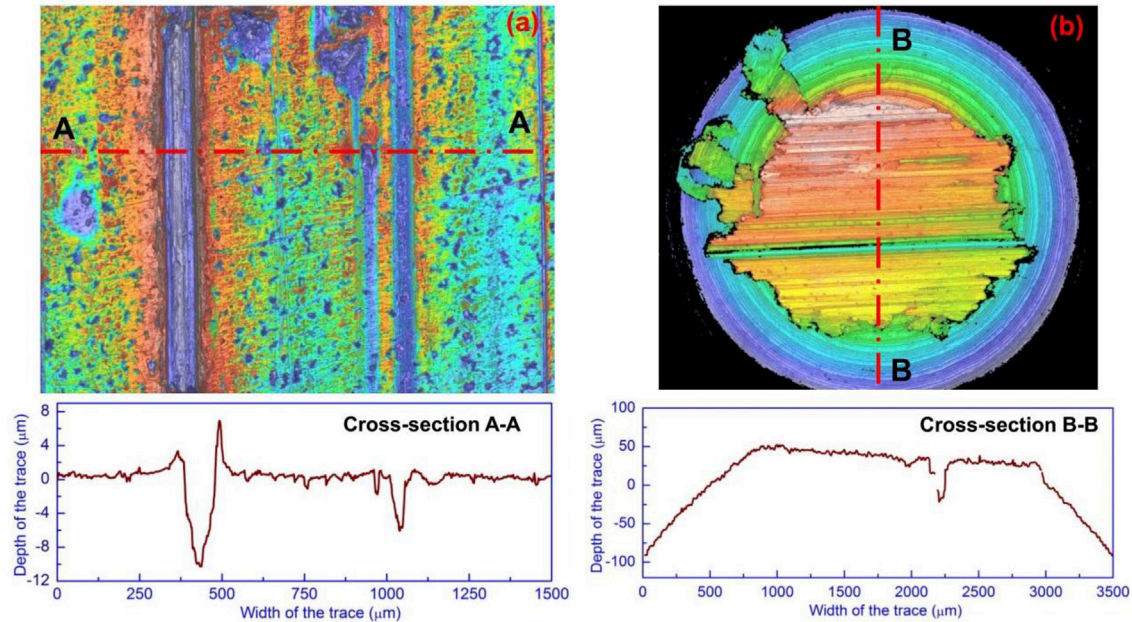
Fig. 11. 3D morphologies and depth profiles of the worn samples: (a). plate sample; (b). pin sample.

reverse trend was observed. Because of the existing of the oxidation layers, when the 18 N contact force applied, the Rc was nearly to 20 mΩ, but when the sliding started and after four cycles, the Rc decreased sharply to 4.2 mΩ. A good correlation between the CoF and the Rc was found during the cycles between 200 and 700. Even though during that time the contact surfaces started to be seriously worn, the plow phe nomenon between the rough surfaces increased the possibility of contact between asperities. At last, the Rc was kept at around 1 mΩ.

4.4. Wear surface morphology and wear rate evaluation

The 3D morphologies of the wear tracks were observed under laser confocal microscope and the depth profiles were measured (Fig. 11). Series abrasive wear observed both on the pin and plate samples. On the tip of the pin, a flat surface with a radius about 1 mm generated, and the pin had a 0.0014 g mass loss due to wear. The wear rate is 2.73×10^{-4} mm^3/N m. The width of the wear track on the 316L plate is about 1.6 mm, with a surface roughness around 1 μm. Before the tribological test, the pin was perpendicularly fixed against the plate (the cantilever beam was parallel to the plate surface). However, with the wear on the pin tip progressing, the angle between the cantilever beam and the plate changed. As a result, the position of wear track on the plate changed accordingly. So, on the plate, two large grooves with a maximum depth of 10 μm generated due to plowing and cutting processes by the CuCuCr pin. The mass loss of the plate is about 0.0015 g, and the wear rate is 3.28×10^{-4} mm^3/N m. The serious abrasion wear on the plate which mimicked the RF conductors showed that the wear resistivity of 316L against CuCrZr under ITER applica tion conditions was poor. As the RF conductors are large components with low maintainability, 316L is unsuitable to be directly applied as the contact material against the RF contact louvers that are made of CuCrZr.

5. Conclusion

A pin on flat type of multifunctional tribometer with linear recipro cating sliding motion scheme was developed on which the ITER ICRH RF contact materials can be researched and validated. The CoF is calculated from the bending strain of a cantilever beam which is measured by using Wheatstone full bridge circuit. The Rc is measured by using four terminal resistance measurements method, and it can be acquired with the CoF simultaneously. The application of dead load loading method can decrease the effects of temperature on the precision of the tribometer, and an innovative loading system was designed to allow gradual increase of the dead loads from outside of the vacuum vessel conveniently. The test samples can be heated up to 250 °C and the whole system can be operated under such temperature steadily. The normal operation vacuum of the HV MTEST is from atmosphere to 10^{-5}Pa (with auxiliary baking). By using FEM, the mechanical designs of the main components were validated. Through calibration, the relationship between the measured strain and the friction force was obtained, which showed a good linear correlation. Based on the HV MTEST system, the performance of material pair (316L versus CuCrZr) foreseen for ITER ICRH RF contact develop ment was studied. The results showed that, the oxidation layers on the CuCrZr led to higher and unstable Rc values. At high temperature (>100 °C), the Rc was not sensitive to the temperature and normal contact force. During the 2000 cycles of sliding test, the maximum of CoF was found nearly to 0.3, and the Rc was kept at 1mΩ steadily. Serious abrasion damage occurred on the 316L plate, and for the future ITER RF conductor application, Rh which has excellent wear resistance is planned to be electroplated on the 316L surface as wear protection func tional coating.

References

[1] Litaudon X, Bernard J, Colas L, Dumont R, Argouarch A, Bottollier-Curtet H, et al. Physics and technology in the ion-cyclotron range of frequency on Tore Supra and TITAN test facility: implication for ITER. Nucl Fusion 2013;53:083012.
[2] Lamalle P, Beaumont B, Kazarian F, Gassmann T, Agarici G, Ajesh P, et al. Status of the ITER ion cyclotron H&CD system. Fusion Eng Des 2013;88:517–20.
[3] Borthwick A, Agarici G, Davis A, Dumortier P, Durodie F, Fanthome J, et al. Mechanical design features and challenges for the ITER ICRH antenna. Fusion Eng Des 2009;84:493–6.
[4] Ferlay F, Bernard J, Dechelle C, Doceul L, Keller D, Wagrez J, et al. First analysis of remote handling maintenance procedure in the hot cell for the ITER ICH&CD antenna–RVTL replacement. Fusion Eng Des 2013;88:1924–8.

[5] Lamalle P, Beaumont B, Kazarian F, Gassmann T, Agarici G, Ajesh P, et al. Status of the ITER ion cyclotron H&CD system. Fusion Eng Des 2013;88:517 20.

[6] Hillairet J, Argouarch A, Bamber R, Beaumont B, Bernard J-M, Delaplanche J-M, et al. R&D activities on RF contacts for the ITER ion cyclotron resonance heating launcher. Fusion Eng Des 2015;96:477–81.

[7] Calatroni S, Perret R, Vollenberg W. RF contacts for the LHC collimators, nuclear instruments and methods in physics research section a. Accel Spectrom Detect Assoc Equip 2006;566:205–11.

[8] R. D, Modeling of the RF-shield sliding contact fingers for the LHC cryogenic beam vacuum interconnects using implicit and explicit finite element formulations, 2008..

[9] Durashevich G, Cvetkovski V, Jovanovich V. Effect of thermomechanical treatment on mechanical properties and electrical conductivity of a CuCrZr alloy. Bull Mater Sci 2002;25:59–62.

[10] Chatterjee A, Mitra R, Chakraborty A, Rotti C, Ray K. Comparative study of approaches to assess damage in thermally fatigued Cu Cr Zr alloy. J Nucl Mater 2016;474:120–5.

[11] Wikman S, Peacock A, Zlamal O, Oijerholm J, Tahtinen S, Rodig M, et al. Assessment of materials data for blanket materials within the European contribution to ITER. J Nucl Mater 2013;442:S414–9.

[12] Barabash V, Kalinin G, Fabritsiev SA, Zinkle SJ. Specification of CuCrZr alloy properties after various thermo-mechanical treatments and design allowables including neutron irradiation effects. J Nucl Mater 2011;417:904–7.

[13] Morgan L, Shimwell J, Gilbert M. Isotopically enriched structural materials in nuclear devices. Fusion Eng Des 2015;90:79–87.

[14] Hoić M, Hrgetić M, Deur J. Design of a pin-on-disc-type CNC tribometer including an automotive dry clutch application. Mechatronics 2016;40:220–32.

[15] Nevshupa RA, Conte M, Igartua A, Roman E, de Segovia JL. Ultrahigh vacuum system for advanced tribology studies: design principles and applications. Tribol Int 2015;86:28–35.

[16] Kosinskiy M, Ahmed SI-U, Liu Y, Schaefer JA. A compact reciprocating vacuum microtribometer. Tribol Int 2012;56:81–8.

[17] Hasler M, Schindelwig K, Mayr B, Knoflach C, Rohm S, van Putten J, et al. A novel ski–snow tribometer and its precision. Tribol Lett 2016;63:33.

[18] Kalita K, Das N, Boruah P, Sarma U. Design and uncertainty evaluation of a strain measurement system. MAPAN 2016;31:17–24.

[19] Rosol M, Pilat A, Turnau A. Real-time controller design based on NI Compact-RIO. IMCSIT 2010:825–30.

[20] Barabash V. Summary of material data for structural analysis of the ITER vacuum vessel and ports. 2008. ITER– D– 229D7N.

[21] Nicholas T. High cycle fatigue: a mechanics of materials perspective. Elsevier; 2006.

[22] Sghaier RB, Majed N, Dali HB, Fathallah R. High cycle fatigue prediction of glass fiber-reinforced epoxy composites: reliability study. Int J Adv Manuf Technol 2017: 1–15.

[23] Barabash V. Appendix A, materials design limit data. 2013. ITER Technical Document ITER D 222RLN v3.3.

[24] Slade PG. Electrical contacts: principles and applications. CRC Press; 2013.

[25] Yaglioglu O, Hart AJ, Martens R, Slocum AH. Method of characterizing electrical contact properties of carbon nanotube coated surfaces. Rev Sci Instrum 2006;77: 095105.

[26] Belous V, Kalinin G, Lorenzetto P, Velikopolskiy S. Assessment of the corrosion behaviour of structural materials in the water coolant of ITER. J Nucl Mater 1998; 258:351–6.

[27] Zheng JH, Bogaerts W, Lorenzetto P. Erosion–corrosion tests on ITER copper alloys in high temperature water circuit with incident heat flux. Fusion Eng Des 2002;61: 649–57.

[28] Bezzazi M, Khamlichi A, Jabbouri A, Reis P, Davim J. Experimental characterization of frictional behaviour of clutch facings using Pin-on-disk machine. Mater Des 2007; 28:2148–53.